Bio-Synthetic AgO Nanoparticles from Microwave Irradiation Method

K. Ravikodi
Department of Physics, St. Jerome's College, Nagercoil, Tamil Nadu, India.

K. Ramkumar
Department of Chemistry, Scott Christian College, Nagercoil, Tamil Nadu, India.

Abstract – AgO nanoparticles have been successfully prepared by biosynthesis technique from bioplastic extract. X-ray diffraction method has been used for the structural identification. TEM, SEM was performed to investigate the morphology of the AgO nanoparticles. Functional groups were identified by FTIR spectrum and the optical constants have been reckoned and illustrated graphically.

Index Terms – Bioplastic Extract, Silver Nitrate, AgO.

1. INTRODUCTION

Ag nanoparticles are now being developed for various applications in many fields. In biological field Ag nanoparticles are used in antimicrobial agents, wound dressing, labeling agents, drug deliveries, bio-imaging, transfection vectors and so on [1-5]. Ag nanoparticles can be synthesized using various methods which are biological, resistive heating, flash evaporation, laser evaporation, sol-gel methods, sputtering, γ-radiation etc [6-19].

In the present work, the AgO nanoparticles prepared from aqueous solution of silver nitrate using bioplastic extract as a reductant. Further AgO nanoparticles were characterized using XRD, TEM, SEM, FTIR and UV-vis.

2. MATERIALS AND METHODS

Bioplastic's extract [20] was prepared by agitating 10g of well cleaned, crushed bioplastic pieces with 80 ml of aqueous solution. After agitating for 10 minutes the broth was filtered and 20ml of silver nitrate (1M) was added with the solution. Then the mixture was placed under microwave irradiation for 5 minutes. The observed colour change of the reaction mixture to dark brown pointed out the formation of AgO particles. The product was filtered by Wattmann paper and dried at room temperature. The dried product was heated in an oven at 80 degree Celsius for 15 minutes.

3. RESULTS AND DISCUSSION

3.1. X-Ray Diffraction Analysis

Based on the XRD pattern, the prepared sample was found to exhibit crystalline nature. The reckoned average grain size (3.7960 nm) using Scherrer's formula and microstrain (Ɛ) by $\beta / 4 \tan \theta$ (0.29590) were compared with grain size (3.6383 nm) and microstrain (0.3048) from Williamson-Hall (W-H) plot. Both the results were approximately equal to each other. Using Cellcalc software the lattice parameters were reckoned and compared with the standard values and is shown in table 1.

Property	Reckoned	Standard	Error
a	5.94606	5.852	0.09406
b	3.52667	3.478	0.04867
c	5.41488	5.495	0.08012
β	109.507	107.50	2.007
Volume	107.031	106.66	0.371
Residual	0.00000735	---	---
Lattice	---	Primitive	---
Space group	---	P21/C	---
System	---	Monoclinic	---

Table 1 Comparison of Standard and Reckoned Properties

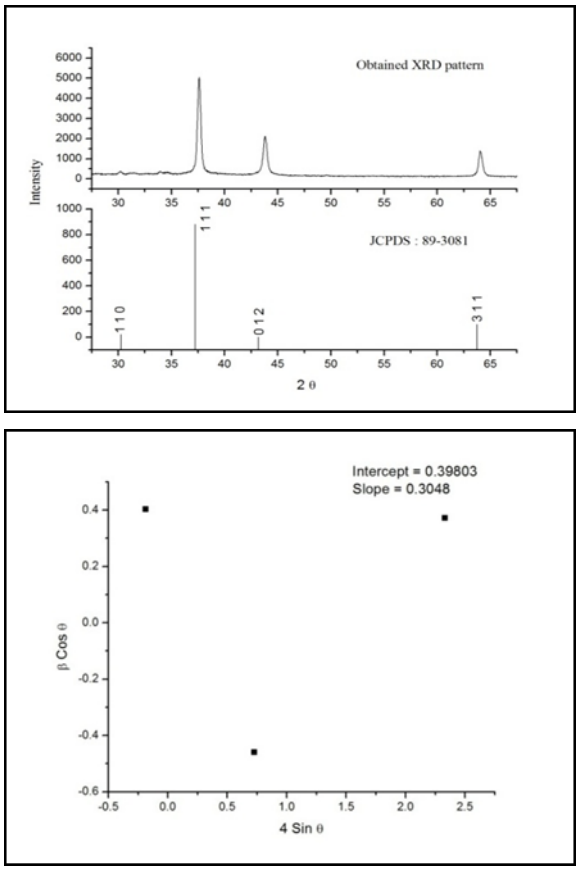

Graph 1: Obtained XRD Pattern and W-H Plot

3.2 TEM Analysis

Figure 1: TEM Image of Prepared AgO Nanoparticles with 100 nm Magnification

The data obtained from transmission electron micrograph showed that the actual shape and size of the nanoparticles in nanometer. The particles were spherical and rodlike in shape in the range of 6 nm to 50 nm.

3.3 SEM Analysis

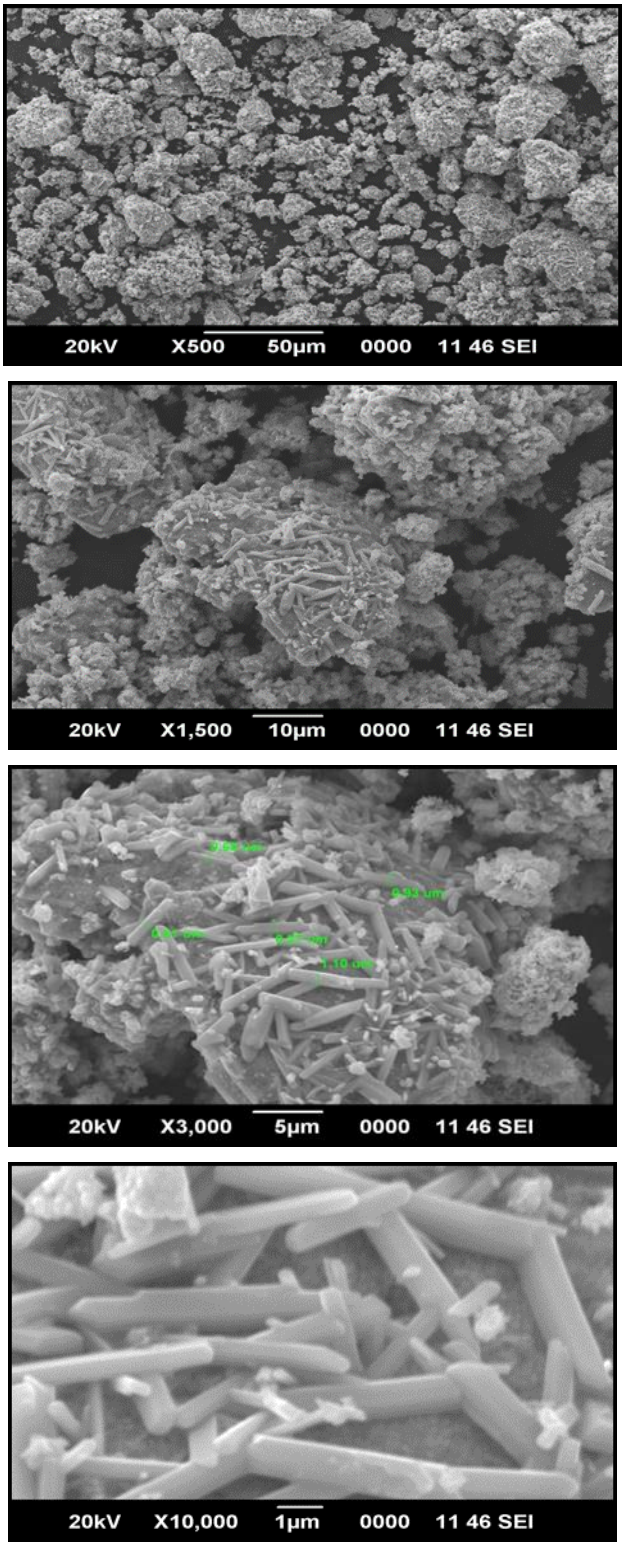

Figure 2: SEM Image of Prepared AgO Nanoparticles for Various Magnification

From the SEM images, the prepared AgO nanoparticles comply with rodlike microstructure. Rodlike nanoparticles are formed during the reduction of metal salts by weak diminishing agents. By this reason the growth occurs over a longer period. The size of these particles ranges from 0.61 µm to 1.10 µm which ratifies their nanostructure. From XRD measurements, the average grain size was 3.796 nm. This is smaller than grain sizes observed by SEM investigation. The observed difference can be attributed to a possible plasmon interaction of SEM electron bundle with Ag-nano particle surface, which appears in magnification size effect.

3.4 FTIR Analysis

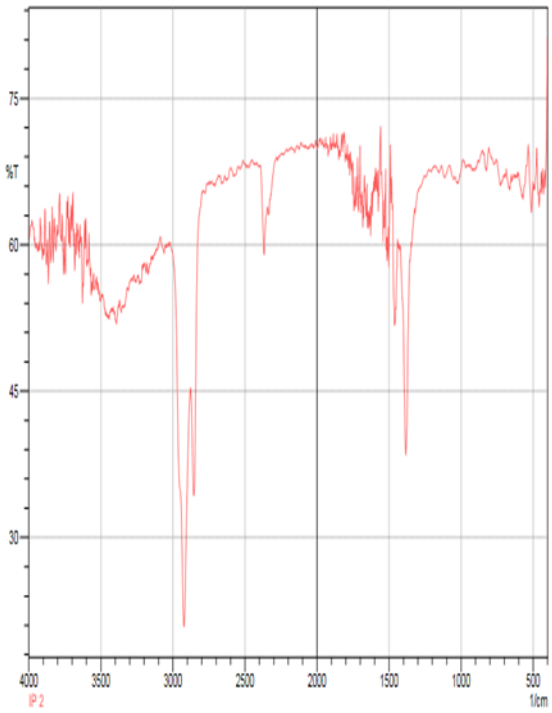

Figure 3: FTIR Data of Prepared AgO Nanoparticles

The peaks 538 cm^{-1} to 1000 cm^{-1} denotes the presence of C-H bending as well as metal oxides. The absorption peak at 1020 cm^{-1} denote C-N stretching, 1382 cm^{-1} denote C-H cellulose, hemicelluloses content, 1494 cm^{-1} denote C-H stretching and 1504 cm^{-1} indicate C=C stretching. The prominent peak at 1650 cm^{-1} describes the presence of N-H bending. The absorption of CO_2 indicated by the peaks 2349 cm^{-1}. The peak at 2854 cm^{-1} assigned to C-H stretching and 2924 cm^{-1} denote the appearance of CH_2 stretching. A broad peak 3000 cm^{-1} to 3600 cm^{-1} indicates the O-H stretch [21-27].

3.5 Optical Studies

The optical absorption co-efficient reckoned from the absorbance spectra of UV using the relation

$$\alpha = \frac{2.303 \log(\frac{I}{I_0})}{d}$$

Where I/I_0 is the absorbance and d is the thickness of the sample. From graph, it can be seen that the optical absorption decreases exponentially below 378 nm and from the Tauc plot, the bandgap is found as 2.893 eV.

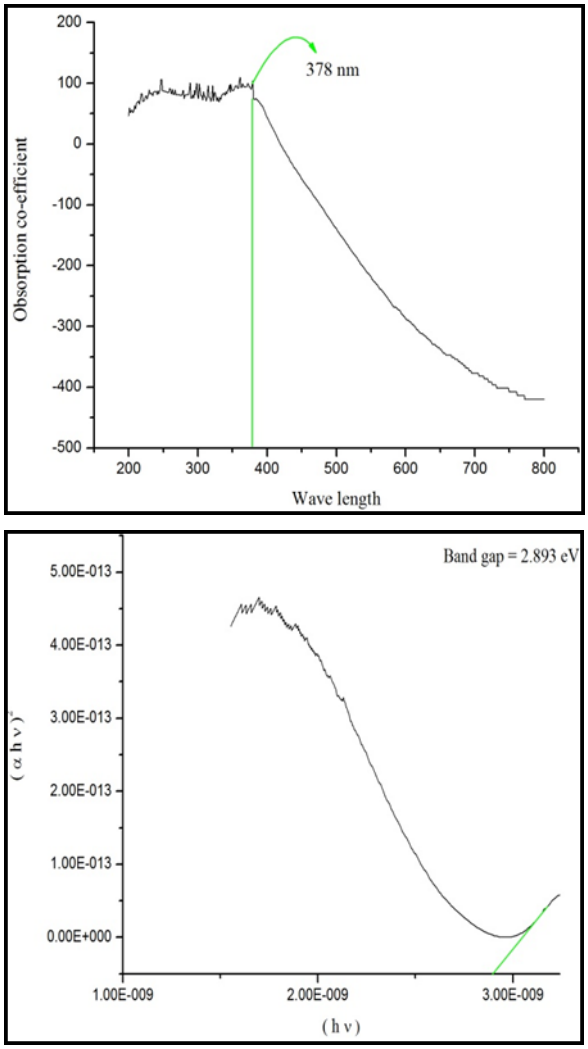

Graph 2: Optical Absorption Co-Efficient Versus Wavelength and Tauc Plot

Extinction Co-efficient was used to measure the light loss due to absorption, scattering and it can be reckoned using the formula,

$$K = \frac{\lambda \alpha}{4 \pi}$$

Where, λ - be the wavelength, α - denotes the obsorption coefficient. From the graph it has been found that extinction co-efficient decreases with the increase of wavelength.

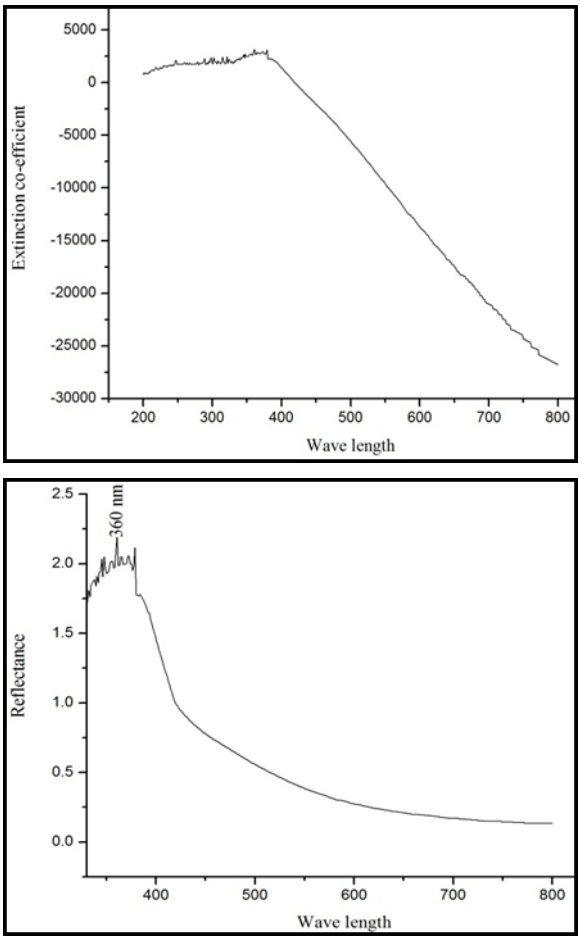

Graph 3: Extinction Co-Efficient and Reflectance Versus Wavelength

The reflectance gives the ratio of the energy reflection of incident light. It can be reckoned using the formula,

$$R = \frac{1 \pm \sqrt{\exp(-\alpha t) + \exp(\alpha t)}}{1 + \exp(-\alpha t)}$$

Where, α - be the obsorption coefficient and t - represents the thickness. The peak value of reflectance (2.193) occurs in the UV region at 360 nm. The speed of light in a substance is measured by refractive index of the substance. The refractive index has been calculated by using the relation,

$$n = \frac{-(R+1) \pm \sqrt{-3R^3 + 10R - 3}}{2(R-1)}$$

Where, R is the reflectance. The average value of refractive index in the visible region is 2.03. This means, electromagnetic radiation is 2.03 times slower in AgO nanoparticles than in free space [28].

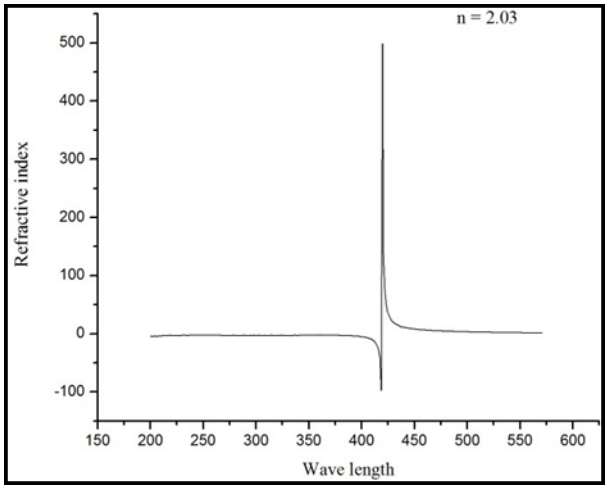

Graph 4: Refractive Index Versus Wavelength

4. CONCLUSION

XRD pattern exhibits the sample's crystalline nature. Structural identifications are reckoned and compared with standard values then the errors were founded out. From morphological study AgO nanoparticles were comply with spherical and rodlike structure. The absorption peaks of FTIR describes about the functional groups of the prepared sample. The optical characterization shows that the bandgap of AgO nanoparticle was 2.893 eV, refractive index reckoned as 2.03 and obsorption co-efficient, extinction co-efficient, reflectance decreases with increase of wavelength.

REFERENCES

[1] Tiwari DK, Behari J, Sen P (2008) Time and dose dependent antimicrobial potential of Ag- nanoparticle synthesized by top-down approach. Curr Sci. 95:1–10.
[2] Chen J, Han CM, Lin XW, Tang ZJ, Su SJ (2006) Effect of silver nanoparticle dressing on second degree burn wound. Zhonghua Wai Ke Za Zhi 44: 50–52.
[3] Patel K, Kapoor S, Dave DP, Mukherjee T (2005) Synthesis of Nanosized Silver Colloids by Microwave Dielectric Heating J. Chem. Sci. 117 (1). pp. 53 – 60.
[4] Soppimath KS, Aminabhavi TM, Kulkarni AR, Rudzinski WE (2001) Biodegradable polymeric nanoparticles as drug delivery devices. J Contr Rel. 70:1–20.
[5] Jin T, Fujii F, Komai Y, Seki J, Seiyama A, Yoshioka Y (2000) Preparation and characterizationof highly fluorescent, glutathione-coated near infrared quantum dots for in vivo fluorescence imaging. Int J Mol Sci 9: 2044–2061.
[6] J.F. Pierson and C. Rousselot, "Stability of reactively sputtered silver oxide films", Surface and Coatings Technology, vol. 200, pp. 276-279, 2005.
[7] X.Y. Gao, H.L. Feng, J.M. Ma, Z.Y. Zhang, J.X. Lu, Y.S. Chen, S.E. Yang and J.H. Gu, "Analysis of the dielectric constants of the Ag2O film by spectroscopic ellipsometry and single-oscillator model," Physica B, vol. 405, pp. 1922-1926, 2010.
[8] X.Y. Gao, S.Y. Wang, J. Li, Y.X. Zheng, R.J. Zhang, P. Zhou, Y.M. Yang and L.Y. Chen, "Study of structure and optical properties of silver

oxide films by ellipsometry, XRD and XPS methods," Thin Solid Films, vol. 455-456, pp. 438- 442, 2004.
[9] Y. Chiu, U. Rambabu, M.H. Hsu, H.P.D. Shieh, C.Y. Chen and H.H. Lin, "Fabrication and nonlinear optical properties of nanoparticle silver oxide films", Journal of Applied Physics, vol. 94, pp. 1996-2001, 2003.
[10] M.F. Al-kuhaili, Journal of Physics D: Applied Physics, vol. 40, pp2847-2853, 2007.
[11] S.M. Hou, M. Ouyang, H.F. Chen, W.M. Liu, Z.Q. Xue, Q.D. Wu, H.X. Zhang, H.J. Gao and S.J. Pang, "Fractal structure in the silver oxide thin films," Thin Solid Films, vol. 315, pp. 322-326, 1998.
[12] N. Ravichandra Raju, K. Jagadeesh Kumar and A. Subrahmanyam, "Physical properties of silver oxide thin films by pulsed laser deposition: "Effect of oxygen pressure during growth," Journal of Physics D: Applied Physics, vol. 42, pp.135411-6, 2009.
[13] X.Y. Gao, H.L. Feng, Z.Y. Zhang, J.M. Ma and J.X. Lu, "Effects of rapid thermal processing on microstructure and optical properties of as-deposited Ag2O films by DC reactive magnetron sputtering," Chinese Physics Letters, vol. 27, pp. 026804, 2010.
[14] X.Y. Gao, Z.Y. Zhang, J.M. Ma, J.X. Lu, J.H. Gu and S.E. Yang, "Effect of the sputtering power on the crystalline structure and optical properties of the silver oxide films deposited using DC reactive magnetron sputtering," Chinese Physics B, vol. 20, pp. 026103-6, 2011.
[15] H.L. Feng, X.Y. Gao, Z.Y. Zhang and J.M. Ma, "Study on the crystalline structure and thermal stability of silver-oxide films deposited by using DC reactive 11 magnetron sputtering methods," Journal of Korean Physical Society, vol. 56, pp. 1176-1179, 2010.
[16] H.E. Mehdi, M.R. Hantehzadeh and S. Valedbagi, "Physical properties of silver oxide thin film prepared by DC magnetron sputtering: effect of oxygen partial pressure during growth," Journal of Fusion Energy, vol. 32, pp. 28-33, 2013.
[17] K.M. Zhao, Y. Liang, X.Y. Gao, C. Chen, X.M. Chen and X.W. Zhao, "Evolution of the structural and optical properties of silver oxide films with different stoichiometries deposited by DC magnetron reactive sputtering,"Chinese Physics B, vol. 21, pp. 066101, 2012.
[18] J.F. Pierson, D. Wiederkehr and A. Billard, "Reactive magnetron sputtering of copper, silver and gold", Thin Solid Films, vol. 478, pp. 196-205, 2005.
[19] J.M. Ma, Y. Liang, X.Y. Gao, Z.Y. Zhang, C. Chen, M.K. Zhao, S.E. Yang, J.H. Gu, Y.S. Chen and J.X. Lu, "Effect of substrate temperature on microstructure and optical properties of single phased Ag_2O film deposited by using RF sputtering method," Chinese Physics B, vol. 20, pp. 056102-5, 2011.
[20] C.H.Tsou, "Preparation and Characterization of Bioplastic-Based Green Renewable Composites from Tapioca with Acetyl Tributyl Citrate as a Plasticizer" Materials 2014, 7, 5617- 5632.
[21] M.G.Geethu, P.S.Suchithra, C.H.Aswathy, J.M.Dinesh babu, "Fourier transform infrared spectroscopy analysis of different solvent extracts of water hyacinth (eichhornia carassipes mart solms.) An allelopathic approach", World Journal of Pharmacy and Pharmaceutical Sciences, 2011, 3, 1256-1266.
[22] P.A.Gerakines, W.A.Schutte, J.M.Greenberg, "The Infrared band strengths of H_2O, CO and CO_2 in laboratory simulations of astrophysical ice mixtures", Astrophysics, 1994, 3, 281-294.
[23] O.Seiferth, K.Wotter, B.Dillmann, G.Klivenyi, "IR investigations of CO_2 adsorption on chromia surfaces: Cr2O3 (0001)/Cr (110) versus polycrystalline α - Cr_2O_3", Surface Science, 1999, 421, 176-190.
[24] G.A.Baratta, M.E.Ppalumbo, G.Strazzulla, "Simultaneous UV-and ion processing of astrophysically relevant ices", Interstellar and Circumstellar Matter, 2014, 561, 9.
[25] M.M.Pavlovic, V.Cosovic, M.G.Palvovic, N.Talijan, V.Bojanic, "Electrical conductivity of Lignocellulose composites loaded with Electrodeposite copper powders", International Journal of Electrochemical Science, 2011, 6, 3812-3829.
[26] A.Bhanu Priya, R.Vinod kumar, P.Gupta, "Synthesis, characterization and antibacterial activity of biodegradable starch/PVA composite films reinforced with celluloic fibre", Carbohydrate Polymers, 2014, 109, 171-179.
[27] A.Samzadeh-Kermani, N.Esfandiary, "Synthesis and Characterization of New Biodegradable Chitosan /Polyvinyl Alcohol/Cellulose Nanocomposite", Advances in Nanoparticles, 2016, 5, 18-26.
[28] C. Besky Job, "Growth, structural, optical, thermal and photo conductivity studies of Potassium Hepta Fluoro Antimonate crystals", Archives of Applied Science Research, 2015, 7 (5):118-128.